Atmos. Chem. Phys. Discuss., 10, 6955–6994, 2010
www.atmos-chem-phys-discuss.net/10/6955/2010/


Atmospheric Chemistry and Physics Discussions

This discussion paper is/has been under review for the journal Atmospheric Chemistry and Physics (ACP). Please refer to the corresponding final paper in ACP if available.

# Chemistry of hydrogen oxide radicals ($HO_x$) in the Arctic troposphere in spring

**J. Mao[1], D. J. Jacob[1,2], M. J. Evans[3], J. R. Olson[4], X. Ren[5], W. H. Brune[6], J. M. S. Clair[7], J. D. Crounse[7], K. M. Spencer[7], M. R. Beaver[7], P. O. Wennberg[8,9], M. J. Cubison[10], J. L. Jimenez[10], A. Fried[11], P. Weibring[11], J. G. Walega[11], S. R. Hall[12], A. J. Weinheimer[12], R. C. Cohen[13], G. Chen[4], J. H. Crawford[4], L. Jaeglé[14], J. A. Fisher[2], R. M. Yantosca[1], P. Le Sager[1,*], and C. Carouge[1]**

[1]School of Engineering and Applied Sciences, Harvard University, Cambridge, MA, USA
[2]Department of Earth and Planetary Sciences, Harvard University, Cambridge, MA, USA
[3]School of Earth and the Environment, University of Leeds, Leeds, LS2 9JT, UK
[4]Science Directorate, NASA Langley Research Center, Hampton, VA, USA
[5]Rosenstiel School of Marine and Atmospheric Science, University of Miami, Miami, FL, USA
[6]Department of Meteorology, Pennsylvania State University, University Park, PA, USA
[7]Division of Chemistry and Chemical Engineering, California Institute of Technology, Pasadena, CA, USA
[8]Division of Geological and Planetary Sciences, California Institute of Technology, Pasadena, CA, USA

[9]Division of Engineering and Applied Science, California Institute of Technology, Pasadena, CA, USA
[10]Department of Chemistry and Biochemistry and Cooperative Institute for Research in the Environmental Sciences (CIRES),University of Colorado at Boulder, Boulder, CO, USA
[11]Earth Observing Laboratory, National Center for Atmospheric Research, Boulder, CO, USA
[12]Atmospheric Chemistry Division, National Center for Atmospheric Research, Boulder, CO, USA
[13]Department of Chemistry and Department of Earth and Planetary Science, University of California Berkeley, Berkeley, CA, USA
[14]Department of Atmospheric Sciences, University of Washington, Seattle, Washington, USA
*now at: KNMI, Chemistry and Climate Division, De Bilt, The Netherlands

Received: 3 March 2010 – Accepted: 4 March 2010 – Published: 11 March 2010

Correspondence to: J. Mao (mao@fas.harvard.edu)

Published by Copernicus Publications on behalf of the European Geosciences Union.





## Abstract

We use observations from the April 2008 NASA ARCTAS aircraft campaign to the North American Arctic, interpreted with a global 3-D chemical transport model (GEOS-Chem), to better understand the sources and cycling of hydrogen oxide radicals ($HO_x \equiv H+OH+peroxy$ radicals) and their reservoirs ($HO_y \equiv HO_x+peroxides$) in the springtime Arctic atmosphere. We find that a standard gas-phase chemical mechanism overestimates the observed $HO_2$ and $H_2O_2$ concentrations. Computation of $HO_x$ and $HO_y$ gas-phase chemical budgets on the basis of the aircraft observations also indicates a large missing sink for both. We hypothesize that this could reflect $HO_2$ uptake by aerosols, favored by low temperatures and relatively high aerosol loadings, through a mechanism that does not produce $H_2O_2$. Such a mechanism could involve $HO_2$ aqueous-phase reaction with sulfate (58% of the ARCTAS submicron aerosol by mass) to produce peroxymonosulfate ($HSO_5^-$) that would eventually convert back to sulfate and return water. We implemented such an uptake of $HO_2$ by aerosol in the model using a standard reactive uptake coefficient parameterization with $\gamma(HO_2)$ values ranging from 0.02 at 275 K to 0.5 at 220 K. This successfully reproduces the concentrations and vertical distributions of the different $HO_x$ species and $HO_y$ reservoirs. $HO_2$ uptake by aerosol is then a major $HO_x$ and $HO_y$ sink, decreasing mean OH and $HO_2$ concentrations in the Arctic troposphere by 48% and 45% respectively. Circumpolar budget analysis in the model shows that transport of peroxides from northern mid-latitudes contributes 50% of the $HO_y$ source above 6 km, and cloud chemistry and deposition of $H_2O_2$ account together for 40% of the $HO_y$ sink below 3 km. Better rate and product data for $HO_2$ uptake by aerosol are needed to understand this role of aerosols in limiting the oxidizing power of the Arctic atmosphere.




ACPD

10, 6955–6994, 2010



## 1 Introduction

Radiative forcing by aerosol and tropospheric ozone pollution transported from mid-latitudes may be an important driver of recent Arctic warming (Quinn et al., 2008; Shindell et al., 2008). This pollution is strongest in spring (Scheuer et al., 2003) and is modulated by chemical reactions serving as sources or sinks of aerosols and ozone. The Arctic photochemical environment in spring is characterized by polar sunrise, low sun angles, intense cold, and underlying ice surface. Considerable attention has focused on halogen radical photochemistry under these conditions as a rapid sink for ozone (Simpson et al., 2007), but this appears to be important only in the shallow boundary layer where sea ice provides a halogen radical source (Wagner et al., 2001). Hydrogen oxide radicals ($HO_x \equiv H+OH+$peroxy radicals) have a more pervasive effect in the tropospheric column but the chemistry of these radials in the Arctic spring has received little study. The OH radical is the principal atmospheric oxidant, affecting both aerosols and ozone in complex ways. Peroxy radical reactions with nitric oxide (NO) are the main chemical source of tropospheric ozone. We use here observations from the April 2008 NASA Arctic Research of the Composition of the Troposphere from Aircraft and Satellites (ARCTAS) aircraft campaign (Jacob et al., 2009), interpreted with a global 3-D chemical transport model (GEOS-Chem CTM), to better understand the sources and cycling of $HO_x$ radicals in the springtime Arctic atmosphere.

$HO_x$ radicals originate from water vapor. The main pathway involves oxidation by the high-energy O ($^1$D) atom produced from photolysis of ozone:

$$O_3 + h\nu \rightarrow O(^1D) + O_2 \quad \text{(R1)}$$

$$O(^1D) + H_2O \rightarrow 2OH \quad \text{(R2)}$$

The OH atoms cycle with peroxy radicals, driving various $HO_x$-catalyzed mechanisms for atmospheric oxidation and ozone formation and loss. Oxidation of methane and other volatile organic compounds (VOCs) yields formaldehyde (HCHO), which photolyzes to produce additional $HO_x$ radicals and amplify the original source:



ACPD
10, 6955–6994, 2010



$$HCHO + h\nu \rightarrow H + HCO \quad \text{(R3)}$$

$$H + O_2 + M \rightarrow HO_2 + M \quad \text{(R4)}$$

$$HCO + O_2 \rightarrow HO_2 + CO \quad \text{(R5)}$$

Loss of $HO_x$ eventually takes place by radical-radical reactions. These reactions can return water vapor in which case the loss is terminal, or they may produce reservoir species such as hydrogen peroxide ($H_2O_2$) and methyl hydrogen peroxide ($CH_3OOH$). The peroxides can photolyze to return $HO_x$ radicals. Alternatively, they can be converted to water or deposited resulting in a terminal $HO_x$ sink. It is useful to define an expanded hydrogen oxides family $HO_y \equiv HO_x$+reservoirs (Jaeglé et al., 2001), where the reservoirs include mainly peroxides but also some other minor reservoir species such as nitrous acid (HONO). The $HO_x$ budget can then be understood on the basis of the $HO_y$ budget and the chemical cycling within the $HO_y$ family, governed in part by reactions involving nitrogen oxide radicals ($NO_x \equiv NO+NO_2$) (Jaeglé et al., 2001). The lifetime of $HO_y$ against conversion to water vapor is of the order of a few days, so that transport of $HO_y$ reservoir species on convective and synoptic scales can modulate the supply of $HO_x$ radicals (Jaeglé et al., 1997; Prather and Jacob, 1997; Müller and Brasseur, 1999).

Past studies of $HO_x$ chemistry in Arctic spring have mainly been from surface sites. They have pointed out the importance of $HO_x$ radical production from photochemically driven snow emissions of $H_2O_2$ (Hutterli et al., 2001; Jacobi et al., 2002, 2004), HCHO (Sumner and Shepson, 1999; Sumner et al., 2002), and HONO (Zhou et al., 2001). They have identified a large photochemical emission of $NO_x$ from snow (Honrath et al., 1999; Ridley et al., 2000) that plays an important role in $HO_x$ cycling (Yang et al., 2002; Chen et al., 2004). Another unique aspect of $HO_x$ chemistry in the boundary layer is the interaction with halogen radicals. These interactions include $HO_x$ production from Br+HCHO (Evans et al., 2003), additional $HO_y$ reservoirs such as HOBr (Bloss et al., 2005), and additional processes for cycling between $HO_2$ and OH (Simpson et al., 2007).





The Arctic boundary layer is very shallow (~100 m) and capped by a strong thermal inversion (Kahl, 1990). The atmosphere above is more relevant for the impacts of $HO_x$ chemistry on the Arctic troposphere. It had received little exploration prior to ARCTAS, due to the requirement of an aircraft with comprehensive chemical payload. The Tropospheric Ozone Production about the Spring Equinox (TOPSE) aircraft campaign conducted a series of flights in the North American Arctic from February to May of 2000 including measurements of total peroxy radicals (Cantrell et al., 2003a), HCHO (Fried et al., 2003), and peroxides (Snow et al., 2003) up to 8 km altitude. Photochemical model calculations constrained with these data found Reactions (R1) and (R3) to be the major $HO_x$ sources (Wang et al., 2003). However, the model greatly overestimated the observed concentrations of peroxy radicals and $H_2O_2$ (Cantrell et al., 2003b; Wang et al., 2003) while underestimating HCHO (Fried et al., 2003).

Observations from the ARCTAS aircraft expand greatly on TOPSE in terms of both coverage and chemical payload. ARCTAS vertical profiles extend from the boundary layer to the stratosphere. The payload included measurements of $HO_x$ radicals by two independent methods to resolve experimental uncertainty (Chen et al., 2010). It also included an extensive suite of $HO_x$ precursors, reservoirs, and related species. As we will see, this ensemble of observations offers strong constraints and a new perspective on the factors controlling $HO_x$ concentrations in the Arctic spring troposphere.

## 2 Data and model

### 2.1 The ARCTAS campaign

The ARCTAS spring campaign took place from 1–21 April 2008 (Jacob et al., 2009). It included a DC-8 aircraft with a detailed chemical and aerosol payload and a P-3 aircraft with a detailed aerosol and radiation payload. Both were based in Fairbanks, Alaska (65 N, 148 W). We focus our attention on the DC-8 chemical data but will also make reference to the P-3 aerosol data. The DC-8 conducted nine flights in the North



ACPD
10, 6955–6994, 2010



American Arctic totaling 73 flight hours. These included sorties out of Fairbanks as well as transit flights to and from Thule, Greenland (77 N, 69 W) and Iqaluit, Nunavut (64 N, 69 W). Almost all the data were collected north of 60 N. All flights included frequent vertical profiling from 100 m to 12 km altitude.

One of the major goals of ARCTAS was to better understand radical photochemistry in the Arctic. The DC-8 payload included measurements of $HO_x$ radicals, $NO_x$ radicals, $H_2O_2$, $CH_3OOH$, $HNO_4$, $O_3$, $H_2O$, VOCs, HCHO, aerosol composition, and photolysis frequencies (Jacob et al., 2009). OH and $HO_2$ concentrations were measured by two independent techniques, Laser Induced Fluorescence (LIF) and Chemical Ionization Mass Spectrometry (CIMS). There were instrumental difficulties with the CIMS $HO_2$ measurement but intercomparison for OH shows a median ratio $(OH)_{CIMS}/(OH)_{LIF}=0.73$ ($R=0.51$), which agrees within the stated accuracies (32% for LIF, 65% for CIMS) (Chen et al., 2010). We rely on the LIF measurements here as they covered 96% of the flight hours. We use 1-min average data with reported accuracies in parentheses: OH (32%), $HO_2$(32%), $H_2O_2$(±(40%+100 pptv)), $CH_3OOH$ (±(40%+50 pptv)), ozone (3%), HCHO (12%±26 pptv), NO (10%±5 pptv), $NO_2$(5%±5 pptv), $HNO_4$(30%±15 pptv). We also make use of fine aerosol data including sulfate (34%) and ammonium (34%). The $NO_2$ LIF measurement includes methylperoxynitrate ($CH_3OONO_2$) decomposing in the inlet and this represents a significant positive artifact in the upper troposphere (Browne et al., 2010). We correct for it here by using local $CH_3OONO_2/NO_2$ ratios from the GEOS-Chem simulation. Mean ratios are 0.03 at 0–3 km, 0.17 at 3–6 km, and 1.4 above 6 km.

Several halogen-catalyzed ozone and mercury depletion events were observed during ARCTAS (Salawitch et al., 2010), but all were confined below 500 m. No obvious signature of either bromine or chlorine radical chemistry was found above 500 m from the measured soluble bromide (Liao et al., 2010), BrO (Neuman et al., 2010) or VOC indicators (Fried et al., 2010). We neglect the effect of halogen chemistry in our modeling of the ARCTAS $HO_x$ data but will comment on its possible role in the boundary layer.



ACPD
10, 6955–6994, 2010



## 2.2 GEOS-Chem model

GEOS-Chem is a global 3-D chemical transport model driven by assimilated meteorological observations from the Goddard Earth Observing System (GEOS-5) of the NASA Global Modeling and Assimilation Office (GMAO) (Bey et al., 2001). We apply here GEOS-Chem version 8-01-04 (http://acmg.seas.harvard.edu/geos/index.html) to simulation of the ARCTAS period (April 2008). The GEOS-5 meteorological data have 6-h temporal resolution (3-h for surface variables and mixing depths) with 0.5°×0.667° horizontal resolution and 72 vertical layers from the surface to 0.01 hPa. We regrid here the meteorological data to 2° latitude×2.5° longitude for input to GEOS-Chem. The model is initialized with a 1-year simulation from January 2007 to January 2008 with 4°×5° resolution, and from January 2008 on with 2°×2.5° resolution. Our analysis of the GEOS-Chem simulation focuses on $HO_x$ chemistry. The same GEOS-Chem simulation is applied in companion papers to interpretation of ARCTAS observations for CO (Fisher et al., 2010a), $SO_2$ and sulfate (Fisher et al., 2010b), carbonaceous aerosols (Wang et al., 2010), methane (Pickett-Heaps et al., 2010), and mercury (Holmes et al., 2010).

We use the standard GEOS-Chem simulation of ozone-$NO_x$-$HO_x$-VOC-aerosol chemistry as described for example by Park et al. (2006). We updated the chemical mechanism with compiled data from the Jet Propulsion Laboratory (Sander et al., 2006) (hereinafter "JPL06") and the International Union of Pure and Applied Chemistry (Atkinson et al., 2006) (hereinafter "IUPAC06"). We implemented the Fast-JX radiative transfer code for calculation of photolysis rate constants (Wild et al., 2000; Bian and Prather, 2002), including updates to absorption cross-sections and quantum yields from JPL06. Total ozone columns used as input to Fast-JX are from daily measurements by the Ozone Monitoring Instrument (OMI) satellite instrument with 1°×1° resolution (ftp://toms.gsfc.nasa.gov/pub/omi/data/ozone/Y2008/). The range of ozone columns during ARCTAS was 380~430 Dobson Units. Surface albedo used in Fast-JX is from the Total Ozone Mapping Spectrometer (TOMS) satellite monthly climatology



ACPD
10, 6955–6994, 2010



with 1°×1.25° resolution (Herman and Celarier, 1997).

A major topic of this paper will be the role of $HO_2$ uptake by aerosol. GEOS-Chem includes a general representation for first-order uptake of gases by aerosols parameterized by a reactive uptake coefficient $\gamma$ and applied to the model aerosol fields (Martin et al., 2003). The standard model includes aerosol uptake of $NO_2$, $NO_3$, and $N_2O_5$ (Jacob, 2000; Evans and Jacob, 2005) and aqueous-phase reaction of $H_2O_2$ with $SO_2$ in cloud (Park et al., 2004). Earlier versions also included aerosol uptake of $HO_2$ (Martin et al., 2003a), but this was removed in v7-04-06 (and hence in the v8-01-04 version we used) on the basis of laboratory data indicating low $\gamma$ values in the absence of transition metal catalysts (Thornton and Abbatt, 2005; Sauvage et al., 2007). More recent standard versions of GEOS-Chem (v8-02-01 and beyond), developed after this work was initiated, include $HO_2$ uptake following Thornton et al. (2008). As we will show below, the ARCTAS observations suggest an important role for aerosol uptake of $HO_2$ under the cold, low-light, and relatively aerosol-rich conditions of Arctic spring. The GEOS-Chem simulation of aerosols during ARCTAS is evaluated by Fisher et al. (2010b) and Wang et al. (2010). It provides in general a good match to observations.

Anthropogenic emissions in GEOS-Chem are as described in van Donkelaar et al. (2008). A prominent feature of ARCTAS flights was the influence of Siberian fire plumes (Warneke et al., 2009). Daily biomass burning emissions for 2008 with 1°×1° resolution are specified from the Fire Locating and Monitoring of Burning Emissions (FLAMBE) emission inventory (Reid et al., 2009) constrained by GOES and MODIS fire count data. Further details on model emissions are given by Fisher et al. (2010a).

The model wet deposition scheme is described by Liu et al. (2001). It includes wet scavenging in convective updrafts as well as grid-resolved first-order rainout and washout. Of particular interest here is the representation of peroxide and HCHO scavenging. For warm clouds ($T$ >268 K), $H_2O_2$, $CH_3OOH$, and HCHO are scavenged by liquid water based on their Henry's law constants. For mixed clouds (248 < $T$ <268 K), precipitation is assumed to take place by riming of liquid cloud droplets with retention efficiencies $R_{H_2O_2}$=0.05, $R_{CH_3OOH}$=0.02, and $R_{HCHO}$=0.02 (Mari et al., 2000). In cold



ACPD
10, 6955–6994, 2010



clouds ($T$ <248 K), scavenging of $H_2O_2$ takes place by co-condensation on ice surfaces while scavenging of $CH_3OOH$ and HCHO are considered negligible (Mari et al., 2000).

Dry deposition is calculated using a standard resistance-in-series scheme (Wesely, 1989) applied to the local surface. For snow and ice the deposition velocity of $H_2O_2$ is in the range 0.1–0.3 cm $s^{-1}$, while dry deposition of $CH_3OOH$ and HCHO are negligible. Snow emission could offset dry deposition for the above species (Frey et al., 2005; Frey et al., 2006) but is not taken into account here as its effect would be confined to the shallow boundary layer. For the same reason we find dry deposition to be unimportant from a tropospheric column perspective.

All comparisons between model and observations use model output sampled along the flight tracks and at the flight time with 15-min time resolution. We exclude all measurements in the stratosphere as diagnosed by an ozone/CO molar ratio greater than 1.25. This excludes 72% of the data above 10 km, 41% of the data at 8–10 km, and 9% of the data at 6–8 km. We also exclude all measurements at latitudes lower than 60N. In order to assess the effect of GEOS-Chem errors for species driving $HO_x$ chemistry (such as ozone, CO, NO), we compare results to those of a gas-phase photochemical box model (Olson et al., 2004) constrained locally by the ARCTAS observations (Olson et al., 2010). Similar comparisons between GEOS-Chem and this box model have been conducted in previous aircraft campaigns (Olson et al., 2004; Hudman et al., 2007; Zhang et al., 2008).

Previous comparisons of the GEOS-Chem $HO_x$ simulation to aircraft LIF measurements from the same Pennsylvania State University group have been reported for the NASA INTEX-A campaign over North America (summer 2004) and the NASA INTEX-B campaign over the North Pacific (spring 2006). Hudman et al. (2007) reported a model overestimate of 30~60% for both OH and $HO_2$ in INTEX-A, but subsequent recalibration of the measurements resolved the discrepancy (Ren et al., 2008). Zhang et al. (2008) found no model bias for $HO_2$ in INTEX-B but a 27% high bias for OH. The global mean tropospheric OH concentration in our ARCTAS simulation is $10.3\times10^5$ molecules $cm^{-3}$, consistent with the multimodel annual mean of



ACPD
10, 6955–6994, 2010



$11.1 \pm 1.7 \times 10^5$ molecule $cm^{-3}$ from the intercomparison by Shindell et al. (2006).

## 3 Median distributions

Figure 1 presents median vertical profiles of OH, $HO_2$, $H_2O_2$, $CH_3OOH$, NO, $NO_2$, HCHO and $HNO_4$ concentrations for 1 km vertical bins during ARCTAS. We compare here the observed profiles (black) to results from the standard GEOS-Chem simulation not including $HO_2$ uptake by aerosols (dashed green line). Also shown in Fig. 1 are model simulations including $HO_2$ uptake, which will be discussed in Sect. 4. Most data were collected under sunlit conditions, between 08:00 and 18:00 local time. Stratospheric data were excluded as described in Sect. 2. Mean observed temperature is 256 K at 0–3 km, 243 K at 3–6 km, and 226 K above 6 km, consistent with the model.

Observed concentrations of OH are relatively low (20 ppqv=$5 \times 10^5$ molecules $cm^{-3}$ in surface air) reflecting the low water vapor, low solar elevation, and thick ozone columns characteristic of Arctic spring. The model reproduces the observed OH concentrations including the vertical gradient with no significant bias.

Observed concentrations of $HO_2$, $H_2O_2$, and $CH_3OOH$ show little altitude dependence, consistent with TOPSE (Wang et al., 2003) but in contrast to measurements in the tropics and northern mid-latitudes that show decreases with altitude driven by water vapor (Cohan et al., 1999; O'Sullivan et al., 1999; Hudman et al., 2007; Snow et al., 2007; Zhang et al., 2008). The model reproduces this lack of vertical structure in the Arctic spring observations and attributes it to a strong vertical gradient of UV radiation (low solar angles, thick ozone columns) compensating for the water vapor gradient and the influx of peroxides from northern mid-latitude into upper troposphere.

The standard simulation overestimates $HO_2$ and $H_2O_2$ by up to a factor of 2. Olson et al. (2010) find a similar discrepancy for $HO_2$ in their box model results, and show that it cannot be resolved by adjusting observed concentrations of other species (such as NO or BrO) within their measurement uncertainties. A similar overestimate of $HO_2$ and $H_2O_2$ was previously found in TOPSE when comparing box model calculations to



ACPD
10, 6955–6994, 2010



observations (Cantrell et al., 2003b; Wang et al., 2003). We propose below that aerosol uptake of $HO_2$ leading to a terminal sink for $HO_y$ could be particularly efficient in the Arctic and explain the discrepancy between model and observations.

Median observed $NO_x$ concentrations increase from 13 pptv in the boundary layer to 21 pptv in the upper troposphere. The model is consistent, increasing from 16 pptv in the boundary layer to 33 pptv in the upper troposphere. April observations from TOPSE at 60–80 N showed a mean NO concentration of 6 pptv (Wang et al., 2003), consistent with the ARCTAS observations and with the model. A sensitivity model simulation with no fuel emissions shows a 40% mean decrease of $NO_x$ along the ARCTAS flight tracks, while a sensitivity simulation with no biomass burning emissions shows only a 5% decrease. We conclude that a large fraction of the $NO_x$ in ARCTAS was anthropogenic.

Peroxynitric acid ($HNO_4$) is an important reservoir for $HO_x$ in the upper troposphere at northern mid-latitudes (Jaeglé et al., 2001). ARCTAS observations are below the detection limit in the lower troposphere due to thermal dissociation but increase to 30 pptv in the upper troposphere. The model reproduces the observed concentrations and vertical gradient within the measurement uncertainty.

Observed HCHO decreases with altitude, from 140 pptv near the surface to 25 pptv in the upper troposphere. TOPSE observations by a similar absorption spectrometer using a tunable lead-salt diode laser averaged 95 pptv below 0.2 km and 60 pptv at 6–8 km (Fried et al., 2003). A different laser source, based on tunable difference frequency generation (DFG), was employed in ARCTAS (Weibring et al., 2007; Richter et al., 2009). Model values decrease from 50 pptv near the surface to 30 pptv in the upper troposphere. The discrepancy below 3 km is outside the stated precision of the measurements (26 pptv). Olson et al. (2010) find a similar discrepancy in their box model simulation of the ARCTAS data (with the point-by-point median discrepancies range up to 75 pptv for altitudes between 0.5 and 3 km), and Fried et al. (2003) also reported a low model bias relative to the TOPSE data. Previous GEOS-Chem evaluation with observed HCHO vertical profiles at northern mid-latitudes using a tunable lead-salt diode laser by the same investigator show no such discrepancy (Palmer et al.,



ACPD
10, 6955–6994, 2010



2003; Millet et al., 2006). Halogen radial chemistry and snow emissions of HCHO could provide additional HCHO that is not included in the model at perhaps altitudes as high as 0.5 km. However, this does not explain discrepancies between 0.5 and 3 km given the lifetime of HCHO (hours). Singh et al. (2000) suggested a heterogeneous conversion from $CH_3OH$ to HCHO, but we find no correlation between these two species below 4 km ($R$ <0.01). Although these discrepancies are small, it is important that they are resolved. Fried et al. (2010) will further discuss this. As pointed out in Sect. 5, the source of $HO_x$ and $HO_y$ implied by the observed HCHO appears inconsistent with independent calculations of $HO_x$ and $HO_y$ sinks from the ARCTAS observations.

## 4 $HO_2$ uptake by aerosols

### 4.1 Parameterization of uptake

A prominent feature of the comparison between model and observations in Fig. 1 is the overestimate of $HO_2$. Such a discrepancy has been reported in a number of previous model studies and tentatively attributed to $HO_2$uptake by aerosols (Cantrell et al., 1996a, 1996b; Plummer et al., 1996; Jaeglé et al., 2000; Kanaya et al., 2000; Sommariva et al., 2004; de Reus et al., 2005; Sommariva et al., 2006). This uptake has been reported in a number of laboratory studies but rates and mechanism are uncertain (Jacob, 2000). It could be particularly important in the Arctic because of the low temperature, relatively high aerosol, and slow photochemical cycling.

Figure 2 summarizes literature data of the $\gamma(HO_2)$ reactive uptake coefficient $\gamma(HO_2)$ for different surface types. $\gamma(HO_2)$ is defined as the fraction of $HO_2$ collisions with the aerosol surface resulting in reaction. Consistently high values ($\gamma(HO_2)$> 0.2) are observed for Cu-doped aqueous surfaces. Soluble copper is known to drive rapid catalytic conversion of $\gamma(HO_2)$ to $H_2O_2$ by redox chemistry (Jacob, 2000). Other values for aqueous surfaces at room temperature are also relatively high ($\gamma(HO_2)$ in the range 0.07–0.2) except for concentrated $H_2SO_4$ ($\gamma(HO_2)$< 0.01). However, $\gamma(HO_2)$ for con-



ACPD
10, 6955–6994, 2010



centrated $H_2SO_4$ increases rapidly with decreasing temperature and exceeds 0.2 at 240 K. Reactive uptake coefficients in general increase with decreasing temperature, reflecting negative temperature dependences of both the mass accommodation coefficient $\alpha$ on the surface and the solubility constant (Kolb et al., 1995). Solid surfaces do not take up $HO_2$ significantly. To our knowledge no data are available for $\gamma(HO_2)$ on organic surfaces.

A high reactive uptake probability ($\gamma(HO_2)>0.1$) is needed for aerosol uptake to compete in the atmosphere with other chemical sinks for $HO_x$. This requires that the aerosol be aqueous. Relative humidity (RH) relative to liquid water was typically in the range 40–80% during ARCTAS. Aerosol measurements aboard the P-3 show that non-refractory submicron particles contributed more than 90% of total surface area (McNaughton et al., 2010). High-resolution Aerosol Mass Spectrometer (AMS; DeCarlo et al., 2006) measurements aboard the DC-8 show an average mass composition for non-refractory submicron particles of 58% sulfate, 32% organic aerosol, 6% ammonium, 3% nitrate, and 0.7% chloride (Cubison et al., 2008). An ammonium vs. sulfate molar plot for the AMS data (Fig. 3) shows dominance of the acidic $NH_4HSO_4$ form, although in some cases the aerosol was close to sulfuric acid while in other cases it was fully neutralized as $(NH_4)_2SO_4$. Because of metastability of the aqueous phase, both $NH_4HSO_4$ and $(NH_4)_2SO_4$ are expected to remain aqueous over the range of RH values experienced in ARCTAS (Onasch et al., 1999; Martin et al., 2003b; Colberg et al., 2004). Sulfuric acid is aqueous under all conditions. In addition, Parsons et al. (2004) found that the crystallization RH of ammonium sulfate aerosol decreases as the organic fraction increases. We assume therefore that the aerosol surface area in ARCTAS was mainly contributed by aqueous particles.

To investigate the role of $HO_2$ uptake by aerosol in our ARCTAS simulations, we included the $\gamma(HO_2)$ parameterization of Thornton et al. (2008) as implemented in the most recent standard versions of GEOS-Chem (v8-02-01 and beyond). This parameterization describes $HO_2$ uptake by aqueous aerosol as driven by acid-base dissociation followed by the $HO_2(aq)+O_2^-$ reaction at an assumed pH 5, producing $H_2O_2$ that



ACPD
10, 6955–6994, 2010



then volatilizes to the gas phase. It is clearly inconsistent with the prevailing acidic conditions observed in ARCTAS (Fig. 3), and is also theoretically incorrect since it describes $HO_2$ uptake as a second-order process while the $\gamma(HO_2)$ parameterization intrinsically describes a first-order process. Nevertheless, as shown in Fig. 2 (solid line), it yields values of $\gamma(HO_2)$, that are consistent with those measured in the laboratory for acidic surfaces, ganging from less than 0.05 near the surface to 0.4 in the upper troposphere. Its temperature dependence (mainly driven by the Henry's law constant for $HO_2$) is consistent with the laboratory data for concentrated $H_2SO_4$ (Fig. 2). We adopt the Thornton et al. (2008) scheme here to compute $\gamma(HO_2)$ for want of anything better and because it fits the overall laboratory data for acid aerosols.

The fate of $HO_2$ in aerosol phase is generally assumed to involve conversion to $H_2O_2$ followed by $H_2O_2$ volatilization (Jacob, 2000). However, this would exacerbate the overestimate of $H_2O_2$ in ARCTAS (Fig. 1). One possible solution would be protonation of $H_2O_2$ to $HOOH_2^+$ , a very strong oxidant (Oiestad et al., 2001), which would rapidly react and convert to $H_2O$. However, this requires normal acidity (pH<0) to be effective (Bach and Su, 1994). Such a mechanism could conceivably take place in concentrated $H_2SO_4$ aerosols, but not in the less acidic aerosol that prevailed under ARCTAS conditions (Fig. 3).

Another possible solution is that $HO_2$ uptake may not produce $H_2O_2$. Cooper and Abbatt (1996) proposed that $HO_2$ could react with $HSO_4^-$, forming the peroxymonosulfate radical $SO_5^-$:

$$HO_2 + HSO_4^- \rightarrow SO_5^- + H_2O \qquad \text{(R6)}$$

The possible atmospheric chemistry of the $SO_5^-$ radical is discussed by Jacob (1986), who proposed that the dominant sinks would be the exothermic reactions with $O_2^-$, $HCOO^-$, and $HSO_3^-$, all producing the peroxide $HSO_5^-$ (peroxymonosulfate). Peroxymonosulfate is the first dissociated form of Caro's acid ($H_2SO_5$, highly hygroscopic solid at room temperature, melting point 45 °C), which has first and second acid dissociation constants ($pK_a$) of 0.4 and 9.1 (Elias et al., 1994). As a peroxide, $HSO_5^-$ is a member



ACPD
10, 6955–6994, 2010



of the $HO_y$ family and so its formation does not necessarily represent a terminal sink of $HO_x$. However, Jacob (1986) suggested that the subsequent fate of $HSO_5^-$ in an acidic environment might follow Reactions (R7) and (R8), terminally losing $HO_y$ by conversion to water:

$$HSO_5^- + OH \rightarrow SO_5^- + H_2O \quad \text{(R7)}$$

$$HSO_5^- + HSO_3^- + H^+ \rightarrow 2SO_4^{2-} + 2H^+ \quad \text{(R8)}$$

Another possible mechanism for uptake of $HO_2$ by sulfate aerosols might involve the formation of an $HO_2$ complex. Miller and Francisco (2001) found from quantum chemical calculations that a stable $HO_2$-$H_2SO_4$ complex can be formed in the gas as well as in the aerosol phase. $HSO_4^-$ has similar potential for bonding with $HO_2$ molecules (C. Miller, personal communication, 2009). The fate of these complexes is unknown. They must not decompose to the original reactants if they are to represent an actual $HO_x$ or $HO_y$ sink. One possibility would be conversion to $SO_5^-$ by Reaction (R6), with subsequent chemistry forming $HSO_5^-$ and eventually returning water as described above.

### 4.2 Application to the ARCTAS simulation

Figure 1 shows the results of two simulations, one with $HO_2$ aerosol uptake producing $H_2O_2$ ($\gamma(HO_2 \rightarrow 0.5H_2O_2)$, dashed blue line), and the other with $HO_2$ aerosol uptake leading to a permanent $HO_y$ sink as postulated above ($\gamma(HO_2 \rightarrow$products), red line). The first simulation worsens the overestimate of $H_2O_2$, as aerosol uptake now competes with other $HO_x$ sinks such as $OH+HO_2$ and $CH_3O_2+HO_2$ that do not produce $H_2O_2$. The correction to $HO_2$ is also insufficient in the upper troposphere as $H_2O_2$ can be recycled to $HO_x$ by photolysis. The second simulation provides a much better fit to the observations for both $HO_2$ and $H_2O_2$ (within their measurement uncertainties), and



ACPD
10, 6955–6994, 2010



also improves the fit for OH and $CH_3OOH$, while not significantly affecting the fits for the other species. OH concentrations decrease by up to 58% in the upper troposphere.

Figure 4 shows scatterplots of simulated vs. observed OH, $HO_2$, $H_2O_2$, and $CH_3OOH$ concentrations for the model simulation with $\gamma(HO_2 \rightarrow \text{products})$ and the ensemble of tropospheric observations in ARCTAS. The slopes of the reduced-major-axis regression lines are within the measurement accuracy for all species. Correlation coefficients for OH ($R$=0.61) and $HO_2$ ($R$=0.81) are only slightly improved from the gas-phase-only simulation ($R$=0.58 and $R$=0.78 respectively). Correlations are weak for $H_2O_2$($R$=0.45) and $CH_3OOH$ ($R$=0.50), which might reflect the narrow dynamic range. The $HO_2$ variability is mostly correlated with solar zenith angle in both the observations and the model ($R$=−0.80 in both cases), with additional significant correlations with water vapor ($R$=0.30 observed, $R$=0.40 model) and temperature ($R$=0.30 observed, $R$=0.40 model) above 4 km. The correlation of $HO_2$ concentrations with temperature offers some supporting evidence for a sink from aerosol uptake. The DC-8 did not include measurements of aerosol surface area that we could correlate to $HO_2$ concentrations, but in the model we find that temperature is a much stronger driver of $\gamma(HO_2)$ variability than aerosol surface area. No correlation is found between $HO_2$ and $NO_x$ concentrations in either the model or the observations.

## 5 Budget of $HO_x$ radicals in Arctic spring

We now proceed to quantify the budgets of $HO_x$ and $HO_y$ in Arctic spring as constrained by the ARCTAS observations and derived from the model. We use for that purpose the model including terminal loss of $HO_y$ from reactive uptake of $HO_2$ by aerosols as described in Sect. 4.1. Even though the process is uncertain, it represents our best hypothesis for explaining the $HO_x$ and peroxide observations in ARCTAS.

Figure 5 shows the median vertical profiles of $HO_x$ sources and sinks computed from the observed ARCTAS concentrations, gas-phase reaction rate constants from JPL06 and IUPAC06, and $\gamma$ ($HO_2 \rightarrow$ products) from Thornton et al. (2008). The $CH_3O_2$ con-



ACPD
10, 6955–6994, 2010



centration is assumed to be 30% of that of $HO_2$on the basis of the model $HO_2/CH_3O_2$ ratio. $HO_2$ aerosol uptake is computed using local model values for $\gamma$ and aerosol surface area. O ($^1$D)+$H_2O$ and HCHO photolysis are the major $HO_x$ sources below 4 km. Above that altitude the photolysis of $H_2O_2$ becomes dominant, a remarkable feature that has not been reported to our knowledge anywhere else in the troposphere. It reflects the low OH concentrations in Arctic spring and therefore the dominance of photolysis as a $H_2O_2$ sink rather than reaction with OH (Fig. 5).

The $HO_2$+$HO_2$ reaction is the principal $HO_x$ sink in the lower troposphere but $HO_2$ uptake by aerosol becomes dominant above 5 km. $HO_x$ sinks from $CH_3O_2$ + $HO_2$ and OH+$HO_2$ are relatively small. The $NO_x$-based $HO_x$ sinks including $HO_2$+$NO_2$, OH+$HNO_4$, and OH+$NO_2$ are negligibly small because of the low $NO_x$ concentrations, so that ozone production is $NO_x$-limited throughout the troposphere (Jaeglé et al., 2001). In contrast, previous aircraft campaigns at northern mid-latitudes (SONEX, INTEX-A) found that the $NO_x$-based reactions dominated the $HO_x$ sink in the upper troposphere, implying $NO_x$-neutral or $NO_x$-saturated conditions for ozone production (Jaeglé et al., 2000; Ren et al., 2008). The observed $NO_x$ concentrations in the upper troposphere in these campaigns (medians of 93 pptv in SONEX, 440 pptv in INTEX-A) are much higher than in ARCTAS (33 pptv), reflecting major sources at northern mid-latitudes from convective injection of pollution and lightning (Jaeglé et al., 1998; Allen et al., 2000; Hudman et al., 2007).

We see from Fig. 5 that $HO_2$ uptake by aerosols is crucial for balancing the $HO_x$ sources with the $HO_x$ sinks independently computed from observations, at least in the upper troposphere. There the main gas-phase sinks ($HO_2$+$HO_2$, $CH_3O_2$+$HO_2$, OH+$HO_2$) can balance only 20% of the $HO_x$ source. With $HO_2$ uptake by aerosol included in the budget, the total $HO_x$ sinks balance 50% of the $HO_x$ sources in the lower troposphere and 70% in upper troposphere. The imbalance in the lower troposphere reflects the high observed HCHO concentrations (Fig. 1), for which we have no explanation. The aerosol sink is ineffective in the lower troposphere because of the relatively high temperatures (average $T$=258 K at 0–2 km, resulting in $\gamma(HO_2)$=0.06).

Figure 5 also shows the median vertical profiles of instantaneous $HO_y$ source and sink terms, again computed from the measurements. The main $HO_y$ sources are O($^1$D)+$H_2O$ and HCHO photolysis. The main sinks are $HO_2$ uptake by aerosol and the gas-phase OH+$CH_3OOH$ reaction. OH+$H_2O_2$ is relatively unimportant due to its much slower rate constant ($1.8\times10^{-12}$ cm$^3$ molecules$^{-1}$ s$^{-1}$, no temperature dependence) compared to OH + $CH_3OOH$ ($3.8\times10^{-12}$ exp(200/T) cm$^3$ molecules$^{-1}$ s$^{-1}$) as given by JPL06. Such a dominance of the gas-phase $HO_y$ sink by the OH+$CH_3OOH$ reaction has not been reported before to our knowledge, except in deep convective outflow where $H_2O_2$ has been scavenged but not $CH_3OOH$ (Cohan et al., 1999). We attribute it to the low concentrations of $NO_x$ in Arctic spring, suppressing the $NO_x$-based $HO_x$ sinks (see discussion above) and promoting $CH_3OOH$ formation.

Figure 5 shows an imbalance between $HO_y$ chemical sources and sinks that reverses sign with altitude. The $HO_y$ sink balances 30% of the source below 3 km, 92% at 3–6 km, and 170% above 6 km. The $HO_y$ lifetime is 2–6 d, sufficiently long that additional terms may be relevant in the $HO_y$ budget including long-range transport, wet and dry deposition, and aqueous-phase oxidation of $SO_2$ by $H_2O_2$ in clouds. To consider the effect of these terms, we conducted a $HO_y$ budget analysis in the GEOS-Chem model averaged over the 60–90 N circumpolar Arctic cap. Results are shown in Fig. 6. The budget in the model is balanced by mass conservation; the excess of $HO_y$ sources over $HO_y$ sinks in the tropospheric column reflects accumulation of peroxides over the course of April.

We see from Fig. 6 that influx of peroxides from northern mid-latitudes in the model accounts for 50% of the total $HO_y$ source above 6 km and 20% at 3–6 km. This explains the chemical imbalance in the $HO_y$ budget constrained by the ARCTAS observations (Fig. 5). Considering the dominant role of $H_2O_2$ photolysis as a source of $HO_x$ above 5 km (Fig. 5), this implies a significant contribution of northern mid-latitudes to the $HO_x$ budget of the Arctic free troposphere. Below 3 km, we find in the model that cloud chemistry and deposition of $H_2O_2$ together account for 40% of the $HO_y$ sink. This helps but is insufficient to correct the chemical imbalance in the $HO_y$ budget constrained by



ACPD
10, 6955–6994, 2010



the observations. As in the case of the $HO_x$ budget, the residual imbalance reflects the high observed HCHO.

Figure 7 gives a summary diagram of the $HO_x$ and $HO_y$ cycling as represented by our model for Arctic spring. Primary sources include the O ($^1$D)+$H_2O$ reaction within the region (70%) and transport of peroxides from northern mid-latitudes (30%). Photolysis of HCHO produced from oxidation of methane by OH is a major amplifying source of $HO_y$, of comparable magnitude to the primary source from O ($^1$D)+$H_2O$. $HO_2$ aerosol uptake accounts for 35% of the $HO_y$ sink. Cycling within the $HO_x$ family (between OH and peroxy radicals) is relatively efficient (chain length=3.4) given the low $NO_x$ concentrations. This is because formation of peroxides to terminate the chain is slow as a result of the low $HO_x$ concentrations.

## 6 Implications

The ARCTAS observations show a large missing sink of $HO_x$ and $HO_y$ in Arctic spring relative to current understanding. If our hypothesis that this reflects a fast terminal loss of $HO_2$ to aerosols is correct, then it implies a significant sensitivity of the oxidizing power of the Arctic atmosphere to aerosol perturbations. A measure of this effect is provided by the difference in Fig. 1 between our standard simulation (solid red line) and the gas-only simulation (dashed green line). In the absence of aerosols, OH and $HO_2$ concentrations would increase on average respectively by 48% and 45% in the tropospheric column, the largest effects being in the upper troposphere where uptake by aerosol is particularly efficient (low temperatures).

Laboratory data show a wide range for the reactive uptake coefficient $\gamma(HO_2)$, as summarized in Fig. 2. Values are generally high for aqueous surfaces and appear to have a strong temperature dependence. Both of these factors are important for $HO_2$ uptake in the Arctic and require further study. In particular, we have no information on $HO_2$ uptake by organic aerosol.





The $HO_2$ chemistry in the aerosol phase is another critical issue to resolve. The only product study to our knowledge is that of Loukhovitskaya et al. (2009), who found $H_2O_2$ to be the main product for solid NaBr surfaces. It is conventionally assumed that uptake by aqueous aerosols would also produce $H_2O_2$ from the $HO_2(aq)+O_2^-$ self-reaction (Thornton et al., 2008) or from catalytic cycles involving transition metal ions (Graedel et al., 1986). We find that an $HO_2$ uptake mechanism producing $H_2O_2$ would greatly overestimate the observed $H_2O_2$ concentrations in ARCTAS. In order to fit the observations, we propose an alternate mechanism involving reaction of $HO_2$ with acid sulfate to produce peroxymonosulfate ($HSO_5^-$). This mechanism and its sensitivity to aerosol acidity need to be tested in the laboratory. $HO_2$ uptake by aerosols has opposite effects on $H_2O_2$ depending on whether $H_2O_2$ is produced or not as a result of uptake. Changes in aerosol types (biomass burning vs. fossil fuel) or aerosol acidity (sulfuric acid vs. ammonium) could thus have large effects on $H_2O_2$. This may be relevant to explaining the complex long-term trend of $H_2O_2$ observed in Greenland ice cores (Möller, 1999).

*Acknowledgements.* The authors would like to thank Scot T. Martin, Cameron S. McNaughton, Hongyu Liu, Charles E. Miller, Richard A. Ferrare, Karl D. Froyd and Daniel M. Murphy for helpful discussions. We also would like to thank Yuhang Wang for providing TOPSE dataset, Huisheng Bian for providing Fast-JX updates and Dirk Richter for contributing to HCHO measurement. J. Mao also thanks David M. Shelow and the NASA DC-8 crew for their generous help with making $HO_x$ measurements on the aircraft. This work was supported by the NASA Tropospheric Chemistry Program.

## References

Allen, D., Pickering, K., Stenchikov, G., Thompson, A., and Kondo, Y.: A three-dimensional total odd nitrogen ($NO_y$) simulation during sonex using a stretched-grid chemical transport model, J. Geophys. Res.-Atmos., 105, 3851–3876, 2000.

Atkinson, R., Baulch, D. L., Cox, R. A., Crowley, J. N., Hampson, R. F., Hynes, R. G., Jenkin, M. E., Rossi, M. J., Troe, J., and IUPAC Subcommittee: Evaluated kinetic and photochemical





data for atmospheric chemistry: Volume II –gas phase reactions of organic species, Atmos. Chem. Phys., 6, 3625–4055, 2006, http://www.atmos-chem-phys.net/6/3625/2006/.

Bach, R. D. and Su, M. D.: The transition-state for the hydroxylation of saturated-hydrocarbons with hydroperoxonium ion, J. Am. Chem. Soc., 116, 10103–10109, 1994.

Bey, I., Jacob, D. J., Yantosca, R. M., Logan, J. A., Field, B. D., Fiore, A. M., Li, Q. B., Liu, H. G. Y., Mickley, L. J., and Schultz, M. G.: Global modeling of tropospheric chemistry with assimilated meteorology: Model description and evaluation, J. Geophys. Res.-Atmos., 106, 23073–23095, 2001.

Bian, H. S. and Prather, M. J.: FAST-J2: Accurate simulation of stratospheric photolysis in global chemical models, J. Atmos. Chem., 41, 281–296, 2002.

Bloss, W. J., Lee, J. D., Johnson, G. P., Sommariva, R., Heard, D. E., Saiz-Lopez, A., Plane, J. M. C., McFiggans, G., Coe, H., Flynn, M., Williams, P., Rickard, A. R., and Fleming, Z. L.: Impact of halogen monoxide chemistry upon boundary layer OH and $HO_2$ concentrations at a coastal site, Geophys. Res. Lett., 32(4), L06814, doi:10.1029/2004GL022084, 2005.

Browne E., Wooldrige, P., and Cohen, R.: $\sum$PNs, $CH_3ONO_2$ and $NO_x$ Observations: Comparisons to TOPSE $\sum$PNs/$O_3$, in preparation, 2010.

Cantrell, C. A., Shetter, R. E., Gilpin, T. M., and Calvert, J. G.: Peroxy radicals measured during mauna loa observatory photochemistry experiment 2: The data and first analysis, J. Geophys. Res.-Atmos., 101, 14643–14652, 1996a.

Cantrell, C. A., Shetter, R. E., Gilpin, T. M., Calvert, J. G., Eisele, F. L., and Tanner, D. J.: Peroxy radical concentrations measured and calculated from trace gas measurements in the Mauna Loa observatory photochemistry experiment 2, J. Geophys. Res.-Atmos., 101, 14653–14664, 1996b.

Cantrell, C. A., Edwards, G. D., Stephens, S., Mauldin, L., Kosciuch, E., Zondlo, M., and Eisele, F.: Peroxy radical observations using chemical ionization mass spectrometry during topse, J. Geophys. Res.-Atmos., 108(D6), 8371, doi:10.1029/2002jd002715, 2003a.

Cantrell, C. A., Mauldin, L., Zondlo, M., Eisele, F., Kosciuch, E., Shetter, R., Lefer, B., Hall, S., Campos, T., Ridley, B., Walega, J., Fried, A., Wert, B., Flocke, F., Weinheimer, A., Hannigan, J., Coffey, M., Atlas, E., Stephens, S., Heikes, B., Snow, J., Blake, D., Blake, N., Katzenstein, A., Lopez, J., Browell, E. V., Dibb, J., Scheuer, E., Seid, G., and Talbot, R.: Steady state free radical budgets and ozone photochemistry during TOPSE, J. Geophys. Res.-Atmos., 108(D4), 8361, doi:10.1029/2002jd002198, 2003b.





Chen, G., Davis, D., Crawford, J., Hutterli, L. M., Huey, L. G., Slusher, D., Mauldin, L., Eisele, F., Tanner, D., Dibb, J., Buhr, M., McConnell, J., Lefer, B., Shetter, R., Blake, D., Song, C. H., Lombardi, K., and Arnoldy, J.: A reassessment of $HO_x$ south pole chemistry based on observations recorded during ISCAT 2000, Atmos. Environ., 38, 5451–5461, doi:10.1016/j.atmosenv.2003.07.018, 2004.

Chen, G., Olson, J., and Crawford, J. H.: Intercomparison results during ARCTAS, in preparation, 2010.

Cohan, D. S., Schultz, M. G., Jacob, D. J., Heikes, B. G., and Blake, D. R.: Convective injection and photochemical decay of peroxides in the tropical upper troposphere: Methyl iodide as a tracer of marine convection, J. Geophys. Res.-Atmos., 104, 5717–5724, 1999.

Colberg, C. A., Krieger, U. K., and Peter, T.: Morphological investigations of single levitated $H_2SO_4/NH_3/H_2O$ aerosol particles during deliquescence/efflorescence experiments, J. Phys. Chem. A, 108, 2700–2709, doi:10.1021/jp037628r, 2004.

Cooper, P. L. and Abbatt, J. P. D.: Heterogeneous interactions of OH and $HO_2$ radicals with surfaces characteristic of atmospheric particulate matter, J. Phys. Chem., 100, 2249-2254, 1996.

Cubison, M. J., Sueper, D., Dunlea, E. J., and Jimenez, J. L.: Submicron aerosol composition during the arctas campaign: Arctic haze, biomass burning, and california pollution, EOS Transaction AGU, 89, Fall Meet. Suppl. A11A-0081, 2008.

de Reus, M., Fischer, H., Sander, R., Gros, V., Kormann, R., Salisbury, G., Van Dingenen, R., Williams, J., Zllner, M., and Lelieveld, J.: Observations and model calculations of trace gas scavenging in a dense Saharan dust plume during MINATROC, Atmos. Chem. Phys., 5, 1787–1803, 2005, http://www.atmos-chem-phys.net/5/1787/2005/.

DeCarlo, P. F., Kimmel, J. R., Trimborn, A., Northway, M. J., Jayne, J. T., Aiken, A. C., Gonin, M., Fuhrer, K., Horvath, T., Docherty, K. S., Worsnop, D. R., and Jimenez, J. L.: Field-deployable, high-resolution, time-of-flight aerosol mass spectrometer, Anal. Chem., 78, 8281–8289, doi:10.1021/ac061249n, 2006.

Elias, H., Gotz, U., and Wannowius, K. J.: Kinetics and mechanism of the oxidation of sulfur(IV) by peroxomonosulfuric acid anion, Atmos. Environ., 28, 439–448, 1994.

Evans, M. J., Jacob, D. J., Atlas, E., Cantrell, C. A., Eisele, F., Flocke, F., Fried, A., Mauldin, R. L., Ridley, B. A., Wert, B., Talbot, R., Blake, D., Heikes, B., Snow, J., Walega, J., Weinheimer, A. J., and Dibb, J.: Coupled evolution of $BrO_x$–$ClO_x$-$HO_x$-$NO_x$ chemistry during bromine-





catalyzed ozone depletion events in the arctic boundary layer, J. Geophys. Res.-Atmos., 108(D4), 8368, doi:10.1029/2002jd002732, 2003.

Evans, M. J. and Jacob, D. J.: Impact of new laboratory studies of $N_2O_5$ hydrolysis on global model budgets of tropospheric nitrogen oxides, ozone, and OH, Geophys. Res. Lett., 32, L09813, doi:10.1029/2005gl022469, 2005.

Fisher, J. A., Jacob, D. J., Purdy, M. T., Kopacz, M., Le Sager, P., Carouge, C., Holmes, C. D., Yantosca, R. M., Batchelor, R. L., Strong, K., Diskin, G. S., Fuelberg, H. E., Holloway, J. S., Hyer, E. J., McMillan, W. W., Warner, J., Streets, D. G., Zhang, Q., Wang, Y., and Wu, S.: Source attribution and interannual variability of Arctic pollution in spring constrained by aircraft (ARCTAS, ARCPAC) and satellite (AIRS) observations of carbon monoxide, Atmos. Chem. Phys., 10, 977–996, 2010a, http://www.atmos-chem-phys.net/10/977/2010/.

Fisher J. A., Jacob, D. J., Dibb, J. E., Scheuer E., Jimenez, J. L., and Cubison, M. : Sources and acidity of sulfate-nitrate-ammonium aerosol in the Arctic in spring, in preparation, 2010b.

Frey, M. M., Stewart, R. W., McConnell, J. R., and Bales, R. C.: Atmospheric hydroperoxides in west antarctica: Links to stratospheric ozone and atmospheric oxidation capacity, J. Geophys. Res.-Atmos., 110, D23301, doi:10.1029/2005jd006110, 2005.

Frey, M. M., Bales, R. C., and McConnell, J. R.: Climate sensitivity of the century-scale hydrogen peroxide ($H_2O_2$) record preserved in 23 ice cores from west antarctica, J. Geophys. Res.-Atmos., 111, D21301, doi:10.1029/2005jd006816, 2006.

Fried, A., Wang, Y. H., Cantrell, C., Wert, B., Walega, J., Ridley, B., Atlas, E., Shetter, R., Lefer, B., Coffey, M. T., Hannigan, J., Blake, D., Blake, N., Meinardi, S., Talbot, B., Dibb, J., Scheuer, E., Wingenter, O., Snow, J., Heikes, B., and Ehhalt, D.: Tunable diode laser measurements of formaldehyde during the TOPSE 2000 study: Distributions, trends, and model comparisons, J. Geophys. Res.-Atmos., 108(D4), 8365, doi:10.1029/2002jd002208, 2003.

Fried A., Richter D., Weibring P., Apel, E. C., Gorham, K. A., Walega J., Blake, D. R., Blake, N. J., Orlando, J. J., Weinheimer, A., Knapp, D. J., Huey, L. G., and Meinardi, S.: Airborne Formaldehyde and VOC Measurements during Select Arctic Boundary Layer Runs in the 2008 ARCTAS Study and Estimates of Halogen Atom Mixing Ratios, in preparation, 2010.

Gershenzon, Y. M., Grigorieva, V. M., Ivanov, A. V., and Remorov, R. G.: $O_3$ and OH sensitivity to heterogeneous sinks of $HO_x$ and $CH_3O_2$ on aerosol particles, Faraday Discuss., 100, 83–100, 1995.

Graedel, T. E., Mandich, M. L., and Weschler, C. J.: Kinetic-model studies of atmospheric





droplet chemistry: 2. Homogeneous transition-metal chemistry in raindrops, J. Geophys. Res.-Atmos., 91, 5205–5221, 1986.
Hanson, D. R., Burkholder, J. B., Howard, C. J., and Ravishankara, A. R.: Measurement of OH and $HO_2$ radical uptake coefficients on water and sulfuric-acid surfaces, J. Phys. Chem., 96, 4979–4985, 1992.
Herman, J. R. and Celarier, E. A.: Earth surface reflectivity climatology at 340–380 nm from toms data, J. Geophys. Res.-Atmos., 102, 28003–28011, 1997.
Holmes, C. D., Jacob, D. J., Corbitt E. S., Soerensen, A. L., and Talbot, R.: Global atmospheric budget of mercury including oxidation of elemental mercury by bromine atoms, in preparation, 2010.
Honrath, R. E., Peterson, M. C., Guo, S., Dibb, J. E., Shepson, P. B., and Campbell, B.: Evidence of $NO_x$ production within or upon ice particles in the greenland snowpack, Geophys. Res. Lett., 26, 695–698, 1999.
Hudman, R. C., Jacob, D. J., Turquety, S., Leibensperger, E. M., Murray, L. T., Wu, S., Gilliland, A. B., Avery, M., Bertram, T. H., Brune, W., Cohen, R. C., Dibb, J. E., Flocke, F. M., Fried, A., Holloway, J., Neuman, J. A., Orville, R., Perring, A., Ren, X., Sachse, G. W., Singh, H. B., Swanson, A., and Wooldridge, P. J.: Surface and lightning sources of nitrogen oxides over the united states: Magnitudes, chemical evolution, and outflow, J. Geophys. Res.-Atmos., 112, D12s05, doi:10.1029/2006JD007912, 2007.
Hutterli, M. A., McConnell, J. R., Stewart, R. W., Jacobi, H. W., and Bales, R. C.: Impact of temperature-driven cycling of hydrogen peroxide ($H_2O_2$) between air and snow on the planetary boundary layer, J. Geophys. Res.-Atmos., 106, 15395–15404, 2001.
Hutterli, M. A., McConnell, J. R., Chen, G., Bales, R. C., Davis, D. D., and Lenschow, D. H.: Formaldehyde and hydrogen peroxide in air, snow and interstitial air at south pole, Atmos. Environ., 38, 5439–5450, doi:10.1016/j.atmosenv.2004.06.003, 2004.
Jacob, D. J.: Chemistry of OH in remote clouds and its role in the production of formic-acid and peroxymonosulfate, J. Geophys. Res.-Atmos., 91, 9807–9826, 1986.
Jacob, D. J.: Heterogeneous chemistry and tropospheric ozone, Atmos. Environ., 34, 2131–2159, 2000.
Jacob, D. J., Crawford, J. H., Maring, H., Clarke, A. D., Dibb, J. E., Ferrare, R. A., Hostetler, C. A., Russell, P. B., Singh, H. B., Thompson, A. M., Shaw, G. E., McCauley, E., Pederson, J. R., and Fisher, J. A.: The ARCTAS aircraft mission: design and execution, Atmos. Chem. Phys. Discuss., 9, 17073–17123, 2009,





http://www.atmos-chem-phys-discuss.net/9/17073/2009/.
Jacobi, H. W., Frey, M. M., Hutterli, M. A., Bales, R. C., Schrems, O., Cullen, N. J., Steffen, K., and Koehler, C.: Measurements of hydrogen peroxide and formaldehyde exchange between the atmosphere and surface snow at summit, greenland, Atmos. Environ., 36, 2619–2628, 2002.
Jaeglé, L., Jacob, D. J., Wennberg, P. O., Spivakovsky, C. M., Hanisco, T. F., Lanzendorf, E. J., Hintsa, E. J., Fahey, D. W., Keim, E. R., Proffitt, M. H., Atlas, E. L., Flocke, F., Schauffler, S., McElroy, C. T., Midwinter, C., Pfister, L., and Wilson, J. C.: Observed OH and $HO_2$ in the upper troposphere suggest a major source from convective injection of peroxides, Geophys. Res. Lett., 24, 3181–3184, 1997.
Jaeglé, L., Jacob, D. J., Wang, Y., Weinheimer, A. J., Ridley, B. A., Campos, T. L., Sachse, G. W., and Hagen, D. E.: Sources and chemistry of $NO_x$ in the upper troposphere over the united states, Geophys. Res. Lett., 25, 1705–1708, 1998.
Jaeglé, L., Jacob, D. J., Brune, W. H., Faloona, I., Tan, D., Heikes, B. G., Kondo, Y., Sachse, G. W., Anderson, B., Gregory, G. L., Singh, H. B., Pueschel, R., Ferry, G., Blake, D. R., and Shetter, R. E.: Photochemistry of $HO_x$in the upper troposphere at northern midlatitudes, J. Geophys. Res.-Atmos., 105, 3877–3892, 2000.
Jaeglé, L., Jacob, D. J., Brune, W. H., and Wennberg, P. O.: Chemistry of $HO_x$ radicals in the upper troposphere, Atmos. Environ., 35, 469–489, 2001.
Kahl, J. D.: Characteristics of the low-level temperature inversion along the alaskan Arctic coast, Int. J. Climatol., 10, 537–548, 1990.
Kanaya, Y., Sadanaga, Y., Matsumoto, J., Sharma, U. K., Hirokawa, J., Kajii, Y., and Akimoto, H.: Daytime $HO_2$ concentrations at Oki Island, Japan, in summer 1998: Comparison between measurement and theory, J. Geophys. Res.-Atmos., 105, 24205–24222, 2000.
Kolb, C. E., Worsnop, D. R., Zahniser, M. S., Davidovits, P., Keyser, L. F., Leu, M.-T., Molina, M. J., Hanson, D. R., and Ravishankara, A. R.: Laboratory studies of atmospheric heterogeneous chemistry, in: Progress and problems in atmospheric chemistry, edited by: Baker, J., Advanced series in physical chemistry, 3, 771–875, 1995.
Liao, J., Huey, L. G., Scheuer, E., and Dibb, J. E.: Characterization of soluble bromide measurements during ARCTAS, in preparation, 2010.
Liu, H. Y., Jacob, D. J., Bey, I., and Yantosca, R. M.: Constraints from Pb-210 and Be-7 on wet deposition and transport in a global three-dimensional chemical tracer model driven by assimilated meteorological fields, J. Geophys. Res.-Atmos., 106, 12109–12128, 2001.



ACPD
10, 6955–6994, 2010



Loukhovitskaya, E., Bedjanian, Y., Morozov, I., and Le Bras, G.: Laboratory study of the interaction of $HO_2$ radicals with the NaCl, NaBr, $MgCl_2$ center dot $^6$H(2)O and sea salt surfaces, PCCP Phys. Chem. Chem. Phys., 11, 7896–7905, doi:10.1039/b906300e, 2009.

Mari, C., Jacob, D. J., and Bechtold, P.: Transport and scavenging of soluble gases in a deep convective cloud, J. Geophys. Res.-Atmos., 105, 22255–22267, 2000.

Martin, R. V., Jacob, D. J., Yantosca, R. M., Chin, M., and Ginoux, P.: Global and regional decreases in tropospheric oxidants from photochemical effects of aerosols, J. Geophys. Res.-Atmos., 108(D3), 4097, doi:10.1029/2002jd002622, 2003a.

Martin, S. T., Schlenker, J. C., Malinowski, A., Hung, H. M., and Rudich, Y.: Crystallization of atmospheric sulfate-nitrate-ammonium particles, Geophys. Res. Lett., 30(21), 2102, doi:10.1029/2003gl017930, 2003b.

McNaughton, C. S., Clarke, A. D. , Freitag, S., Kapustin, V. N., Kondo, Y., Moteki, N., Sahu, L. K., Takegawa, N., Schwarz, J. P., Spackman, J. R., Diskin, G. S., Sachse, G. W., Podolske, J. R., Holloway, J., Wisthaler, A., Mikoviny, T., De Gouw, J. A., Warneke, C., Jimenez, J. L., Cubison, M., Howell, S., Middlebrook, A. M., Bahreini, R., Anderson, B., Winstead, E. L., Thornhill, K. L., Lack, D. A., Cozic, J., and Brock, C. A.: Absorbing aerosol in the troposphere of the Western Arctic during the 2008 ARCTAS/ARCPAC airborne field campaigns, in preparation, 2010.

Miller, C. E. and Francisco, J. S.: The formation of a surprisingly stable $HO_2$–$H_2SO_4$ complex, J. Am. Chem. Soc., 123, 10387–10388, 2001.

Millet, D. B., Jacob, D. J., Turquety, S., Hudman, R. C., Wu, S. L., Fried, A., Walega, J., Heikes, B. G., Blake, D. R., Singh, H. B., Anderson, B. E., and Clarke, A. D.: Formaldehyde distribution over North America: Implications for satellite retrievals of formaldehyde columns and isoprene emission, J. Geophys. Res.-Atmos., 111, D24s02, doi:10.1029/2005jd006853, 2006.

Möller, D.: Explanation for the recent dramatic increase of $H_2O_2$ concentrations found in greenland ice cores, Atmos. Environ., 33, 2435–2437, 1999.

Mozurkewich, M., McMurry, P. H., Gupta, A., and Calvert, J. G.: Mass accommodation coefficient for $HO_2$ radicals on aqueous particles, J. Geophys. Res.-Atmos., 92, 4163–4170, 1987.

Müller, J. F. and Brasseur, G.: Sources of upper tropospheric $HO_x$: A three-dimensional study, J. Geophys. Res.-Atmos., 104, 1705–1715, 1999.

Neuman, J. A., Nowak, J. B., Huey, L. G., Burkholder, J. B., Dibb, J. E., Holloway, J. S., Liao, J.,





Peischl, J., Roberts, J. M., Ryerson, T. B., Scheuer, E., Stark, H., Stickel, R. E., Tanner, D. J., and Weinheimer, A.: Bromine measurements in ozone depleted air over the Arctic Ocean, Atmos. Chem. Phys. Discuss., 10, 3827–3860, 2010, http://www.atmos-chem-phys-discuss.net/10/3827/2010/.

O'Sullivan, D. W., Heikes, B. G., Lee, M., Chang, W., Gregory, G. L., Blake, D. R., and Sachse, G. W.: Distribution of hydrogen peroxide and methylhydroperoxide over the pacific and south atlantic oceans, J. Geophys. Res.-Atmos., 104, 5635–5646, 1999.

Oiestad, A. M. L., Petersen, A. C., Bakken, V., Vedde, J., and Uggerud, E.: The oxidative power of protonated hydrogen peroxide, Angew. Chem.-Int. Edit., 40, 1305–1309, 2001.

Olson, J. R., Crawford, J. H., Chen, G., Fried, A., Evans, M. J., Jordan, C. E., Sandholm, S. T., Davis, D. D., Anderson, B. E., Avery, M. A., Barrick, J. D., Blake, D. R., Brune, W. H., Eisele, F. L., Flocke, F., Harder, H., Jacob, D. J., Kondo, Y., Lefer, B. L., Martinez, M., Mauldin, R. L., Sachse, G. W., Shetter, R. E., Singh, H. B., Talbot, R. W., and Tan, D.: Testing fast photochemical theory during trace-p based on measurements of OH, $HO_2$, and $CH_2O$, J. Geophys. Res.-Atmos., 109(16), D15s10, doi:10.1029/2003jd004278, 2004.

Olson, J. R., Crawford, J. H., Chen, G., Brune, W. H., Ren, X., Wennberg, P. O., Fried, A., and Mao, J.: Photochemical Analysis of ARCTAS Observations, in preparation, 2010.

Onasch, T. B., Siefert, R. L., Brooks, S. D., Prenni, A. J., Murray, B., Wilson, M. A., and Tolbert, M. A.: Infrared spectroscopic study of the deliquescence and efflorescence of ammonium sulfate aerosol as a function of temperature, J. Geophys. Res.-Atmos., 104, 21317–21326, 1999.

Palmer, P. I., Jacob, D. J., Fiore, A. M., Martin, R. V., Chance, K., and Kurosu, T. P.: Mapping isoprene emissions over north america using formaldehyde column observations from space, J. Geophys. Res.-Atmos., 108(D6), 4180, doi:10.1029/2002jd002153, 2003.

Park, R. J., Jacob, D. J., Field, B. D., Yantosca, R. M., and Chin, M.: Natural and transboundary pollution influences on sulfate-nitrate-ammonium aerosols in the united states: Implications for policy, J. Geophys. Res.-Atmos., 109, D15204, doi:10.1029/2003jd004473, 2004.

Park, R. J., Jacob, D. J., Kumar, N., and Yantosca, R. M.: Regional visibility statistics in the united states: Natural and transboundary pollution influences, and implications for the regional haze rule, Atmos. Environ., 40, 5405–5423, doi:10.1016/j.atmosenv.2006.04.059, 2006.

Parsons, M. T., Knopf, D. A., and Bertram, A. K.: Deliquescence and crystallization of ammonium sulfate particles internally mixed with water-soluble organic compounds, J. Phys.





Chem. A, 108, 11600–11608, doi:10.1021/jp0462862, 2004.
Pickett-Heaps, C. A., Jacob, D. J., Wecht, K. J., Drevet, J., Diskin, G. S., Wofsy, S. C., Worthy, D. E. J., Kort, E. A., Jimenez, R., Daube, B., and Park., S.: Methane Emissions from the Hudson Bay Lowlands: Interpretation of airborne and surface methane observations, in preparation, 2010.
Plummer, D. A., McConnell, J. C., Shepson, P. B., Hastie, D. R., and Niki, H.: Modeling of ozone formation at a rural site in southern ontario, Atmos. Environ., 30, 2195–2217, 1996.
Prather, M. J. and Jacob, D. J.: A persistent imbalance in $HO_x$ and $NO_x$ photochemistry of the upper troposphere driven by deep tropical convection, Geophys. Res. Lett., 24, 3189–3192, 1997.
Quinn, P. K., Bates, T. S., Baum, E., Doubleday, N., Fiore, A. M., Flanner, M., Fridlind, A., Garrett, T. J., Koch, D., Menon, S., Shindell, D., Stohl, A., and Warren, S. G.: Short-lived pollutants in the Arctic: their climate impact and possible mitigation strategies, Atmos. Chem. Phys., 8, 1723–1735, 2008, http://www.atmos-chem-phys.net/8/1723/2008/.
Reid, J. S., Hyer, E. J., Prins, E. M., Westphal, D. L., Zhang, J. L., Wang, J., Christopher, S. A., Curtis, C. A., Schmidt, C. C., Eleuterio, D. P., Richardson, K. A., and Hoffman, J. P.: Global monitoring and forecasting of biomass-burning smoke: Description of and lessons from the Fire Locating and Modeling of Burning Emissions (FLAMBE) program, IEEE J. Sel. Topics Appl. Earth Observations Remote Sens., 2, 144–162, doi:10.1109/jstars.2009.2027443, 2009.
Remorov, R. G., Gershenzon, Y. M., Molina, L. T., and Molina, M. J.: Kinetics and mechanism of $HO_2$ uptake on solid NaCL, J. Phys. Chem. A, 106, 4558–4565, doi:10.1021/jp013179o, 2002.
Ren, X. R., Olson, J. R., Crawford, J. H., Brune, W. H., Mao, J. Q., Long, R. B., Chen, Z., Chen, G., Avery, M. A., Sachse, G. W., Barrick, J. D., Diskin, G. S., Huey, L. G., Fried, A., Cohen, R. C., Heikes, B., Wennberg, P. O., Singh, H. B., Blake, D. R., and Shetter, R. E.: $HO_x$ chemistry during intex-a 2004: Observation, model calculation, and comparison with previous studies, J. Geophys. Res.-Atmos., 113(13), D05310, doi:10.1029/2007jd009166, 2008.
Richter, D., Fried, A., and Weibring, P.: Difference frequency generation laser based spectrometers, Laser and Photonics Reviews, 3, 343–354, doi:10.1002/lpor.200810048, 2009.
Ridley, B., Walega, J., Montzka, D., Grahek, F., Atlas, E., Flocke, F., Stroud, V., Deary, J., Gallant, A., Boudries, H., Bottenheim, J., Anlauf, K., Worthy, D., Sumner, A. L., Splawn, B.,





and Shepson, P.: Is the arctic surface layer a source and sink of $NO_x$ in winter/spring?, J. Atmos. Chem., 36, 1–22, 2000.

Saathoff, H., Naumann, K. H., Riemer, N., Kamm, S., Mohler, O., Schurath, U., Vogel, H., and Vogel, B.: The loss of $NO_2$, $HNO_3$, $NO_3/N_2O_5$, and $HO_2/HOONO_2$ on soot aerosol: A chamber and modeling study, Geophys. Res. Lett., 28, 1957–1960, 2001.

Salawitch, R. J., Canty, T. P., Kurosu, T. P., Chance, K., Liang, Q., Pawson, S., Liu, X., Huey, L. G., Liao, J., Stickel, R. E., Tanner, D., Dibb, J. E., Weinheimer, A. J., Flocke, F. M., Knapp, D. J., Montzka, D. D., Neuman, J., Simpson, W. R., Donohoue, D., Carlson, D., Blake, D. R., Kinnison, D. E., Tilmes, S., Pan, L., Pierce, R., Hendrick, F., Kreher, K., Wang, Y., Choi, S., and Atlas, E. L.: Airborne, Ground-based, and Satellite Measurements of BrO during ARCTAS and ARCPAC, in preparation, 2010.

Sander, S. P., Finlayson-Pitts, B. J., Friedl, R. R., Golden, D. M., Huie, R. E., Keller-Rudek, H., Kolb, C. E., Kurylo, M. J., Molina, M. J., Moortgat, G. K., Orkin, V. L., Ravishankara, A. R., and Wine, P. H.: Chemical Kinetic and Photochemical Data for Use in Atmospheric Studies, Evaluation Number 15, 2006.

Sauvage, B., Martin, R. V., van Donkelaar, A., Liu, X., Chance, K., Jaeglé, L., Palmer, P. I., Wu, S., and Fu, T.-M.: Remote sensed and in situ constraints on processes affecting tropical tropospheric ozone, Atmos. Chem. Phys., 7, 815–838, 2007, http://www.atmos-chem-phys.net/7/815/2007/.

Scheuer, E., Talbot, R. W., Dibb, J. E., Seid, G. K., DeBell, L., and Lefer, B.: Seasonal distributions of fine aerosol sulfate in the north american arctic basin during TOPSE, J. Geophys. Res.-Atmos., 108(D4), 8370, doi:10.1029/2001jd001364, 2003.

Shindell, D. T., Faluvegi, G., Stevenson, D. S., Krol, M. C., Emmons, L. K., Lamarque, J. F., Petron, G., Dentener, F. J., Ellingsen, K., Schultz, M. G., Wild, O., Amann, M., Atherton, C. S., Bergmann, D. J., Bey, I., Butler, T., Cofala, J., Collins, W. J., Derwent, R. G., Doherty, R. M., Drevet, J., Eskes, H. J., Fiore, A. M., Gauss, M., Hauglustaine, D. A., Horowitz, L. W., Isaksen, I. S. A., Lawrence, M. G., Montanaro, V., Muller, J. F., Pitari, G., Prather, M. J., Pyle, J. A., Rast, S., Rodriguez, J. M., Sanderson, M. G., Savage, N. H., Strahan, S. E., Sudo, K., Szopa, S., Unger, N., van Noije, T. P. C., and Zeng, G.: Multimodel simulations of carbon monoxide: Comparison with observations and projected near-future changes, J. Geophys. Res.-Atmos., 111, D19306, doi:10.1029/2006jd007100, 2006.

Shindell, D. T., Chin, M., Dentener, F., Doherty, R. M., Faluvegi, G., Fiore, A. M., Hess, P., Koch, D. M., MacKenzie, I. A., Sanderson, M. G., Schultz, M. G., Schulz, M., Stevenson, D.





S., Teich, H., Textor, C., Wild, O., Bergmann, D. J., Bey, I., Bian, H., Cuvelier, C., Duncan, B. N., Folberth, G., Horowitz, L. W., Jonson, J., Kaminski, J. W., Marmer, E., Park, R., Pringle, K. J., Schroeder, S., Szopa, S., Takemura, T., Zeng, G., Keating, T. J., and Zuber, A.: A multi-model assessment of pollution transport to the Arctic, Atmos. Chem. Phys., 8, 5353–5372, 2008, http://www.atmos-chem-phys.net/8/5353/2008/.

Simpson, W. R., von Glasow, R., Riedel, K., Anderson, P., Ariya, P., Bottenheim, J., Burrows, J., Carpenter, L. J., Frie, U., Goodsite, M. E., Heard, D., Hutterli, M., Jacobi, H.-W., Kaleschke, L., Neff, B., Plane, J., Platt, U., Richter, A., Roscoe, H., Sander, R., Shepson, P., Sodeau, J., Steffen, A., Wagner, T., and Wolff, E.: Halogens and their role in polar boundary-layer ozone depletion, Atmos. Chem. Phys., 7, 4375–4418, 2007, http://www.atmos-chem-phys.net/7/4375/2007/.

Singh, H., Chen, Y., Tabazadeh, A., Fukui, Y., Bey, I., Yantosca, R., Jacob, D., Arnold, F., Wohlfrom, K., Atlas, E., Flocke, F., Blake, D., Blake, N., Heikes, B., Snow, J., Talbot, R., Gregory, G., Sachse, G., Vay, S., and Kondo, Y.: Distribution and fate of selected oxygenated organic species in the troposphere and lower stratosphere over the Atlantic, J. Geophys. Res.-Atmos., 105, 3795–3805, 2000.

Snow, J. A., Heikes, B. G., Merrill, J. T., Wimmers, A. J., Moody, J. L., and Cantrell, C. A.: Winter-spring evolution and variability of $HO_x$ reservoir species, hydrogen peroxide, and methyl hydroperoxide, in the northern middle to high latitudes, J. Geophys. Res.-Atmos., 108(D4), 8362, doi:10.1029/2002jd002172, 2003.

Snow, J. A., Heikes, B. G., Shen, H. W., O'Sullivan, D. W., Fried, A., and Walega, J.: Hydrogen peroxide, methyl hydroperoxide, and formaldehyde over North America and North Atlantic, J. Geophys. Res.-Atmos., 112, D12S07, doi:10.1029/2006jd007746, 2007.

Sommariva, R., Haggerstone, A.-L., Carpenter, L. J., Carslaw, N., Creasey, D. J., Heard, D. E., Lee, J. D., Lewis, A. C., Pilling, M. J., and Zádor, J.: OH and $HO_2$ chemistry in clean marine air during SOAPEX-2, Atmos. Chem. Phys., 4, 839–856, 2004, http://www.atmos-chem-phys.net/4/839/2004/.

Sommariva, R., Bloss, W. J., Brough, N., Carslaw, N., Flynn, M., Haggerstone, A.-L., Heard, D. E., Hopkins, J. R., Lee, J. D., Lewis, A. C., McFiggans, G., Monks, P. S., Penkett, S. A., Pilling, M. J., Plane, J. M. C., Read, K. A., Saiz-Lopez, A., Rickard, A. R., and Williams, P. I.: OH and $HO_2$ chemistry during NAMBLEX: roles of oxygenates, halogen oxides and heterogeneous uptake, Atmos. Chem. Phys., 6, 1135–1153, 2006,





http://www.atmos-chem-phys.net/6/1135/2006/.
Sumner, A. L. and Shepson, P. B.: Snowpack production of formaldehyde and its effect on the arctic troposphere, Nature, 398, 230–233, 1999.
Sumner, A. L., Shepson, P. B., Grannas, A. M., Bottenheim, J. W., Anlauf, K. G., Worthy, D., Schroeder, W. H., Steffen, A., Domine, F., Perrier, S., and Houdier, S.: Atmospheric chemistry of formaldehyde in the arctic troposphere at polar sunrise, and the influence of the snowpack, Atmos. Environ., 36, 2553–2562, 2002.
Taketani, F., Kanaya, Y., and Akimoto, H.: Kinetics of heterogeneous reactions of $HO_2$ radical at ambient concentration levels with $(NH_4)(2)SO_4$ and NaCl aerosol particles, J. Phys. Chem. A, 112, 2370–2377, doi:10.1021/jp0769936, 2008.
Taketani, F., Kanaya, Y., and Akimoto, H.: Heterogeneous loss of $HO_2$ by KCl, synthetic sea salt, and natural seawater aerosol particles, Atmos. Environ., 43, 1660–1665, doi:10.1016/j.atmosenv.2008.12.010, 2009.
Thornton, J. and Abbatt, J. P. D.: Measurements of $HO_2$ uptake to aqueous aerosol: Mass accommodation coefficients and net reactive loss, J. Geophys. Res.-Atmos., 110, D08309, doi:10.1029/2004jd005402, 2005.
Thornton, J. A., Jaeglé, L., and McNeill, V. F.: Assessing known pathways for $HO_2$ loss in aqueous atmospheric aerosols: Regional and global impacts on tropospheric oxidants, J. Geophys. Res.-Atmos., 113, D05303, doi:10.1029/2007jd009236, 2008.
van Donkelaar, A., Martin, R. V., Leaitch, W. R., Macdonald, A. M., Walker, T. W., Streets, D. G., Zhang, Q., Dunlea, E. J., Jimenez, J. L., Dibb, J. E., Huey, L. G., Weber, R., and Andreae, M. O.: Analysis of aircraft and satellite measurements from the Intercontinental Chemical Transport Experiment (INTEX-B) to quantify long-range transport of East Asian sulfur to Canada, Atmos. Chem. Phys., 8, 2999–3014, 2008, http://www.atmos-chem-phys.net/8/2999/2008/.
Wagner, T., Leue, C., Wenig, M., Pfeilsticker, K., and Platt, U.: Spatial and temporal distribution of enhanced boundary layer bro concentrations measured by the GOME instrument aboard ers-2, J. Geophys. Res.-Atmos., 106, 24225–24235, 2001.
Wang, Y. H., Ridley, B., Fried, A., Cantrell, C., Davis, D., Chen, G., Snow, J., Heikes, B., Talbot, R., Dibb, J., Flocke, F., Weinheimer, A., Blake, N., Blake, D., Shetter, R., Lefer, B., Atlas, E., Coffey, M., Walega, J., and Wert, B.: Springtime photochemistry at northern mid and high latitudes, J. Geophys. Res.-Atmos., 108(D4), 8358, doi:10.1029/2002jd002227, 2003.
Wang., Q., Jacob, D. J., Fisher, J. A., Mao, J., Le Sager, P., Leibensperger, E. M., Carouge, C.,





Kondo, Y., Jimenez, J. L., Cubison, M., Howell, S. G., Freitag, S., Clarke, A. D., McNaughton, C. S., Weber, R., and Apel, E. C.: Sources and Sinks of Carbonaceous Aerosols in the Arctic in Spring, in preparation, 2010.

Warneke, C., Bahreini, R., Brioude, J., Brock, C. A., de Gouw, J. A., Fahey, D. W., Froyd, K. D., Holloway, J. S., Middlebrook, A., Miller, L., Montzka, S., Murphy, D. M., Peischl, J., Ryerson, T. B., Schwarz, J. P., Spackman, J. R., and Veres, P.: Biomass burning in Siberia and Kazakhstan as an important source for haze over the Alaskan Arctic in April 2008, Geophys. Res. Lett., 36, L02813, doi:10.1029/2008gl036194, 2009.

Weibring, P., Richter, D., Walega, J. G., and Fried, A.: First demonstration of a high performance difference frequency spectrometer on airborne platforms, Optics Express, 15, 13476–13495, 2007.

Wesely, M. L.: Parameterization of surface resistances to gaseous dry deposition in regional-scale numerical-models, Atmos. Environ., 23, 1293–1304, 1989.

Wild, O., Zhu, X., and Prather, M. J.: Fast-j: Accurate simulation of in- and below-cloud photolysis in tropospheric chemical models, J. Atmos. Chem., 37, 245–282, 2000.

Yang, J., Honrath, R. E., Peterson, M. C., Dibb, J. E., Sumner, A. L., Shepson, P. B., Frey, M., Jacobi, H. W., Swanson, A., and Blake, N.: Impacts of snowpack emissions on deduced levels of OH and peroxy radicals at summit, greenland, Atmos. Environ., 36, 2523–2534, 2002.

Zhang, L., Jacob, D. J., Boersma, K. F., Jaffe, D. A., Olson, J. R., Bowman, K. W., Worden, J. R., Thompson, A. M., Avery, M. A., Cohen, R. C., Dibb, J. E., Flock, F. M., Fuelberg, H. E., Huey, L. G., McMillan, W. W., Singh, H. B., and Weinheimer, A. J.: Transpacific transport of ozone pollution and the effect of recent Asian emission increases on air quality in North America: an integrated analysis using satellite, aircraft, ozonesonde, and surface observations, Atmos. Chem. Phys., 8, 6117–6136, 2008, http://www.atmos-chem-phys.net/8/6117/2008/.

Zhou, X. L., Beine, H. J., Honrath, R. E., Fuentes, J. D., Simpson, W., Shepson, P. B., and Bottenheim, J. W.: Snowpack photochemical production of HONO: A major source of OH in the arctic boundary layer in springtime, Geophys. Res. Lett., 28, 4087–4090, 2001.



ACPD

10, 6955–6994, 2010



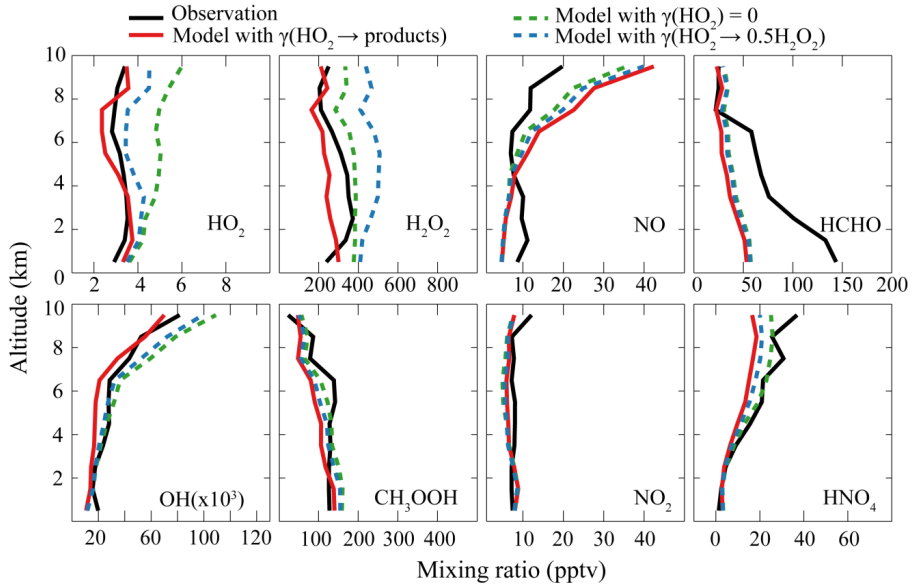


**Fig. 1.** Median vertical profiles of $HO_2$, OH, $H_2O_2$, $CH_3OOH$, NO, $NO_2$, HCHO, and $HNO_4$ concentrations during ARCTAS in the North American Arctic (1–21 April 2008). Observations from the DC-8 aircraft (black lines) are compared to three GEOS-Chem model simulations: (1) without $HO_2$ uptake by aerosol (green dashed line), referred to in the text as "standard GEOS-Chem"; (2) with $HO_2$ uptake yielding $H_2O_2$(blue dashed line); (3) with $HO_2$ uptake not yielding $H_2O_2$ (solid red line). All concentrations are in unit of pptv except OH (ppqv). Most data were collected under sunlit conditions, between 08:00 and 18:00 local time. Stratospheric data were excluded as described in the text.



ACPD
10, 6955–6994, 2010



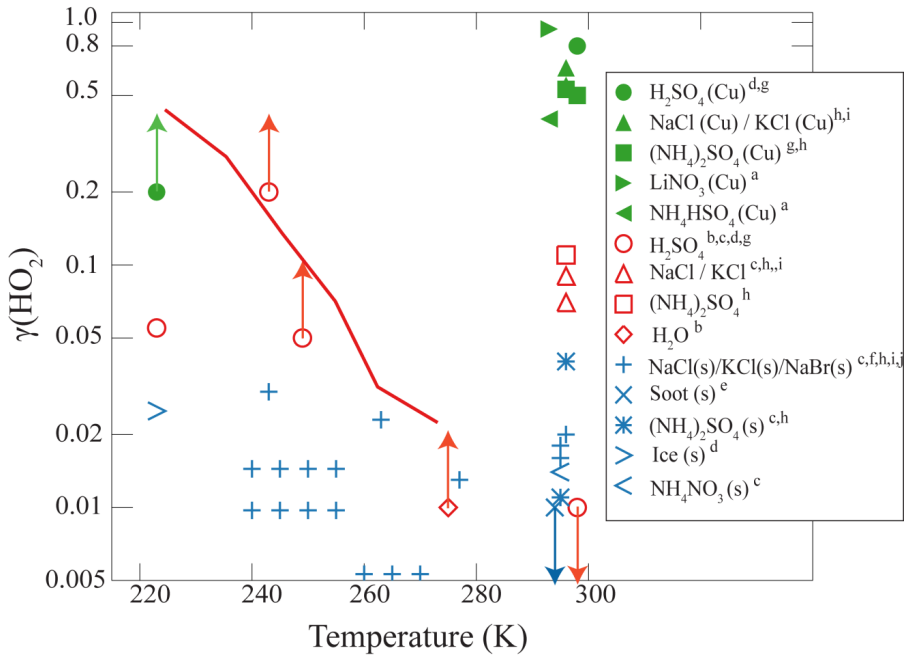


**Fig. 2.** Laboratory data reported in the literature for the reactive uptake coefficient $\gamma$ ($HO_2$) by different surfaces as a function of temperature. Vertical arrows indicate "greater than" or "less than". Open symbols indicate aqueous surfaces, closed symbols indicate copper-doped aqueous surfaces, and other symbols indicate solid surfaces (noted as (s) in the legend). The solid red line is the median value of $\gamma(HO_2)$ computed in GEOS-Chem along the ARCTAS flight tracks using the Thornton et al. (2008) parameterization. Literature references are given by footnotes in legend: **(a)** Mozurkewich et al. (1987); **(b)** Hanson et al. (1992); **(c)** Gershenzon et al. (1995); **(d)** Cooper and Abbatt (1996); **(e)** Saathoff et al. (2001); **(f)** Remorov et al. (2002); **(g)** Thornton and Abbatt (2005); **(h)** Taketani et al. (2008); **(i)** Taketani et al. (2009), **(j)** Loukhovitskaya et al. (2009).



ACPD
10, 6955–6994, 2010



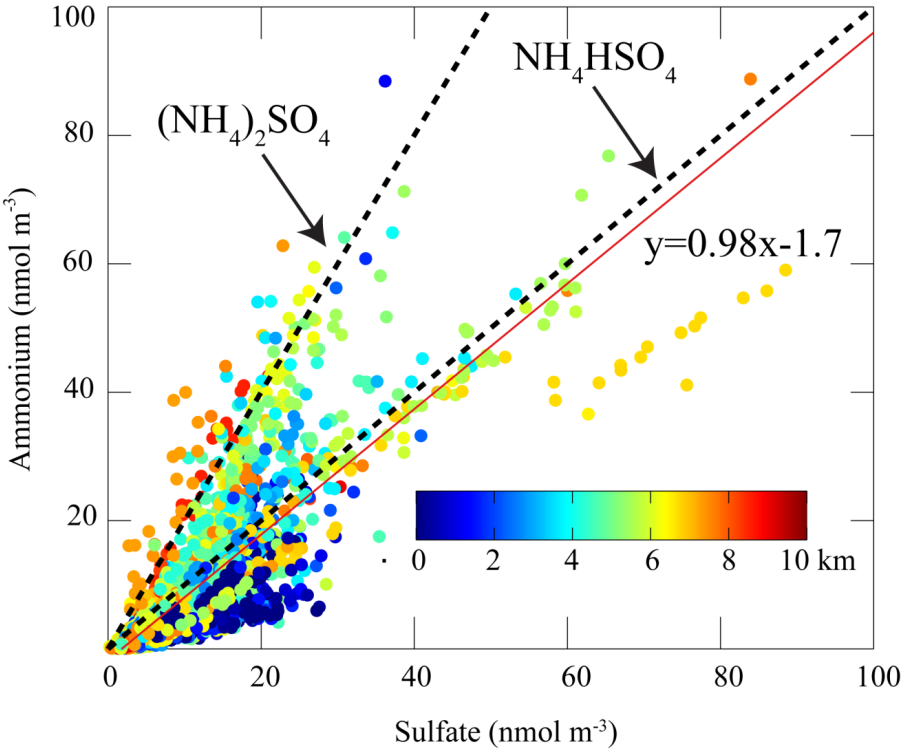


**Fig. 3.** Scatterplot of observed ammonium vs. sulfate submicron aerosol concentrations measured aboard the DC-8 aircraft during ARCTAS-A (April 2008). The observed points are colored by altitude (km). The data from the first two flights (1 and 4 April) are excluded due to low quality of the ammonium data. In red is the linear least squares regression line for all altitudes.



ACPD
10, 6955–6994, 2010



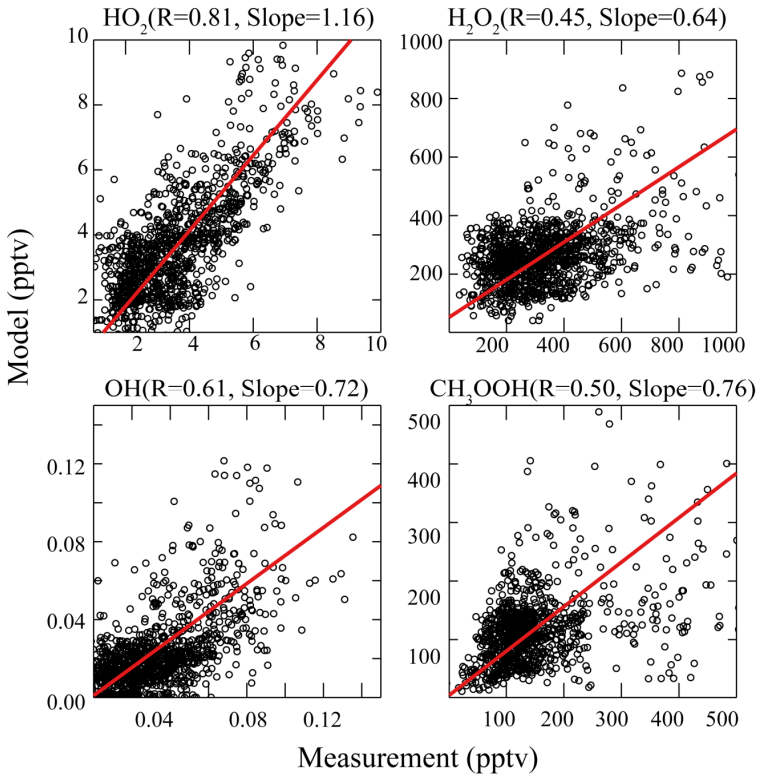


**Fig. 4.** Scatterplots of simulated vs. observed $HO_2$, OH, $H_2O_2$, and $CH_3OOH$ concentrations, for the model simulation with $\gamma(HO_2 \rightarrow \text{products})$ and the ensemble of tropospheric observations during ARCTAS (April 2008). The red solid line is the reduced major axis regression line. Panel titles give the correlation coefficients and regression slopes.



ACPD
10, 6955–6994, 2010



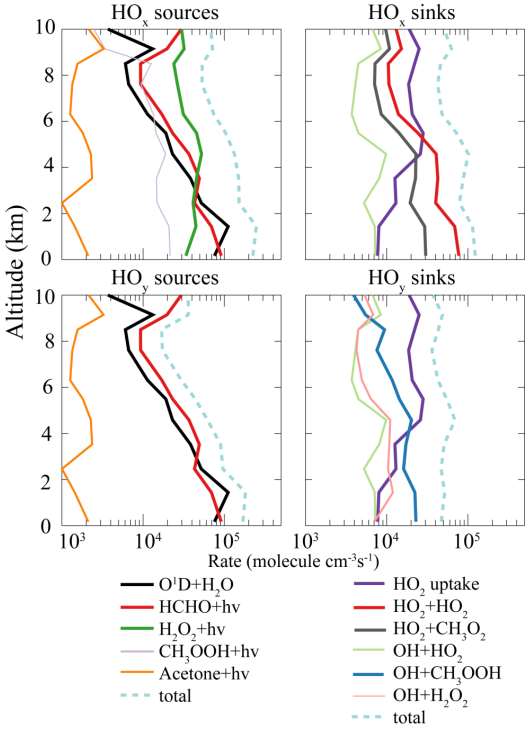


**Fig. 5.** Median vertical profiles of major $HO_x$ and $HO_y$ sources and sinks computed from observed tropospheric concentrations in ARCTAS (April 2008). Values are instantaneous rates. Gas-phase rate constants are from JPL06 and IUPAC06. $HO_2$ uptake by aerosol is computed with a reaction probability $\gamma(HO_2 \rightarrow \text{products})$ from Thornton et al. (2008). Stratospheric data are excluded as described in the text.



ACPD
10, 6955–6994, 2010



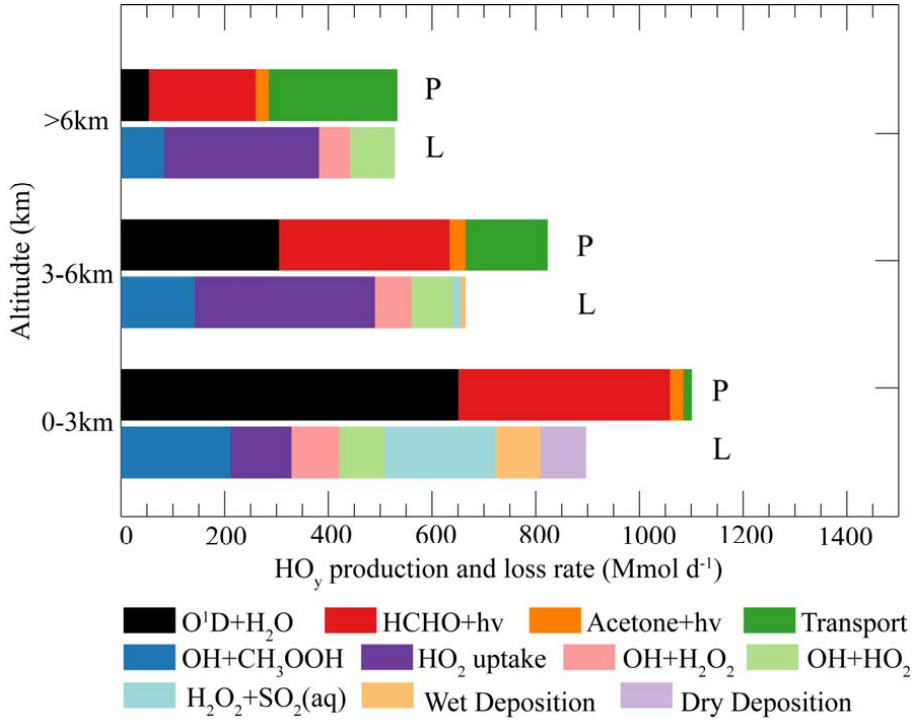


**Fig. 6.** Circumpolar GEOS-Chem model budget of $HO_y$ for the Arctic tropospheric column (60–90 N) during ARCTAS (1–21 April 2008). Mean production rates (P) and loss rates (L) are shown for three altitude bands. The transport term describes exchange with northern mid-latitudes south of 60 N.



ACPD
10, 6955–6994, 2010



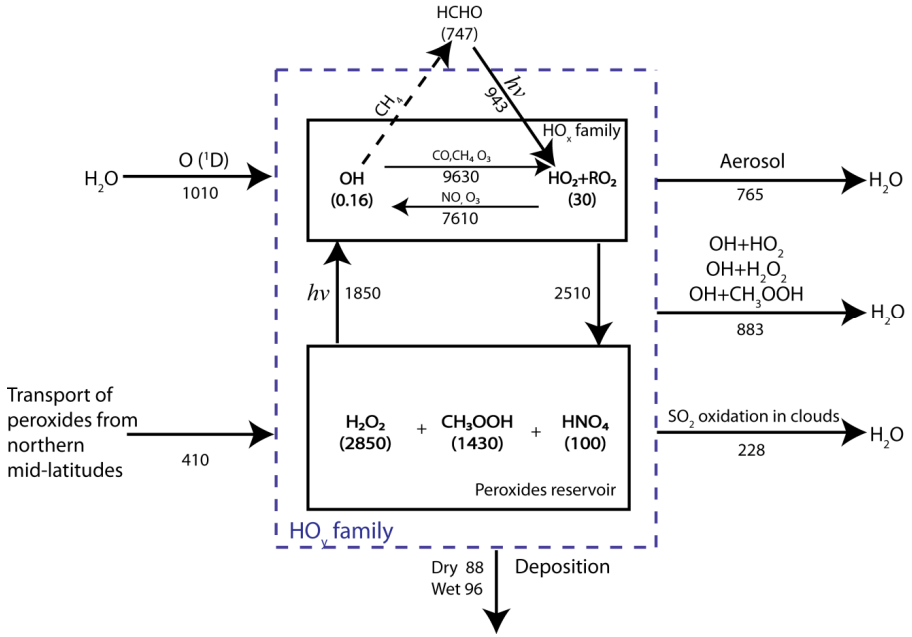


**Fig. 7.** Schematic diagram of $HO_x$-$HO_y$ chemistry in Arctic spring as constructed from the GEOS-Chem model simulation of the ARCTAS observations. Values are tropospheric column averages for April 2008 over the Arctic cap (60–90 N). Masses of chemicals within the domain (in parentheses) are in units of Mmol and rates are in units of Mmol $d^{-1}$. The dashed line for HCHO production indicates that it is not a $HO_y$ sink.